3) The 75 percent BW element design over a quarter-hemisphere maximum VSWR value of 16, and consequently, to be practical, will require an elaborate matching network.

4) It is apparent that, with a careful aperture design, a dual ridge rectangular waveguide offers a practical solution for a wide-band phased array element. This conclusion is confirmed by the results of [7].

5) The present study does not consider the question of polarization. A minor addition to the computer program will yield the axial ratios and the tilt angles.

REFERENCES

[1] S. B. Cohn, "Properties of ridge wave guide," in *Proc. IRE*, pp. 783–788, Aug. 1947.

[2] S. Hopfer, "The design of ridged waveguides," *IRE Trans. Microwave Theory Tech.*, pp. 20–29, Oct. 1955.

[3] J. R. Pyle, "The cutoff wavelength of TE_{10} mode in ridged rectangular waveguide of any aspect ratio," *IEEE Trans. Microwave Theory Tech.*, pp. 175–183, Apr. 1966.

[4] W. J. Getsinger, "Ridge waveguide field description and application to directional couplers," *IRE Trans. Microwave Theory Tech.*, vol. 10, pp. 41–50, Jan. 1962.

[5] J. P. Montgomery, "On the complete eigenvalue solution of ridged waveguide," *IEEE Trans. Microwave Theory Tech.*, pp. 547–555, June 1971.

[6] S. S. Wang, "Wide-Angle wide-band elements for phased arrays," Ph.D. dissertation, Polytechnic Institute of New York, Farmingdale, NY, June 1975.

[7] J. P. Montgomery, "Ridged waveguide-phased array elements," *IEEE Trans. Antennas Propagat.*, vol. AP-24, pp. 46–53, Jan. 1976.

[8] G. V. Borgiotti, "Modal analysis of periodic planar phased arrays of apertures, *Proc. IEEE*, vol. 56, pp. 1881–1892, Nov. 1968.

[9] G. N. Tsandoulas, "Wide-band Limitations of Waveguide Arrays," *Microwave J.*, pp. 49–56, Sept. 1972.

[10] H. Altschuler and L. Goldstone, "On network representations of certain obstacles in waveguide regions," *IRE Trans. Microwave Theory Tech.*, pp. 212–221, Apr. 1959.

[11] N. Marcuvitz, *Waveguide Handbook.* New York: Dover, 1959, p. 57, pp. 218–220.

[12] J. C. Slater, *Microwave Electronics.* Princeton, NJ: D. Van Nostrand, 1959, pp. 80–82.

[13] L. R. Lewis and A. Hessel, "Propagation characteristics of periodic arrays of dielectric slabs," *IEEE Trans. Microwave Theory Tech.*, pp. 96–104, Feb. 1972.

[14] B. L. Diamond and G. H. Knittel: "A new procedure for the design of a waveguide element for a phased array antenna," in *Phased Array Antennas*, A. A. Oliner and G. H. Knittel, Eds. Dedham, MA: Artech House, 1972, pp. 149–156.
B. L. Diamond, "A generalized approach to analysis of infinite planar array antennas", *Proc. IEEE*, pp. 1837–1851. Nov. 1968.

[15] G. F. Farrell and D. H. Kuhn "Mutual coupling in infinite planar arrays of rectangular waveguide horns" *IEEE Trans. Antenna Propagat.*, vol. AP-16, pp. 405–414, July 1968.

The Design of Small Slot Arrays

ROBERT S. ELLIOTT, FELLOW, IEEE, AND L. A. KURTZ

Abstract—**The differences in mutual coupling for a central slot and a peripheral slot cannot be ignored in small arrays if good patterns and impedance are to be obtained. A theory has been developed whereby the length and offset of every slot in the array can be determined, in the presence of mutual coupling, for a specified aperture distribution and impedance match. The theory enlarges on Stevenson's method, and uses a modified form of Booker's relation based on Babinet's principle to treat nonresonant longitudinal shunt slots in the broad wall of a rectangular waveguide. A general relation between slot voltage and mode voltage is developed, and then formulas are derived for the active, self-, and mutual admittances among slots. These formulas result in a design procedure. Analogous treatments of inclined series slots in rectangular guide and of strip-line-fed slots are possible. Comparison between various experiments and the theory is presented. Tests of the theory include the resonant length of a zero offset slot, resonant conductance versus offset and resonant conductance versus frequency for a single slot, and self- and mutual admittances for two staggered slots. The design and performance of a two-by-four longitudinal shunt slot array is also described.**

Manuscript received June 4, 1976; revised May 13, 1977. This work was supported by the Rantec Division, Emerson Electric Company.

R. S. Elliott is with the Department of Electrical Sciences, University of California, Los Angeles, CA 90024, and Consultant to the Rantec Division, Emerson Electric Company, Calabasas, CA 91302.

L. A. Kurtz is with the Rantec Division, Emerson Electric Company, Calabasa, CA, 91302.

THEORY

CONSIDER the module consisting of the solid lines shown in Fig. 1. This is a section of rectangular waveguide $\lambda_g/2$ long containing a longitudinal slot of length $2l$ and displacement x cut in its upper broad wall. One- and two-dimensional slot arrays can be constructed by placing such modules in tandem and parallel positions.

The module of Fig. 1 is a two-port device, the ports being at $z = \pm\lambda_g/4$ if the origin is taken in the waveguide cross section which bisects the slot. But no loss in generality occurs if the ports are taken at the positions $z = \pm\lambda_g$, shown dotted in Fig. 1, because relations between the two sets of ports involve simple known linear transformations. It is convenient to choose the ports at $z = \pm\lambda_g$; with this convention adopted, the equivalent circuit for the nth module[1] is as shown in Fig. 2.

This equivalent circuit is subject to the following interpretation. It is assumed that only the dominant TE_{10} mode can propagate in the waveguide. This mode is represented by the voltage/current pair V_n, I_n at the input port ($z = -\lambda_g$). A load

[1] For notational simplicity the single index n is used to identify this module, but it is important to remember that these modules can be arranged to form either a linear array or a planar array. Double subscript notation could be used in the latter case.

0018-926X/78/0300-0214$00.75

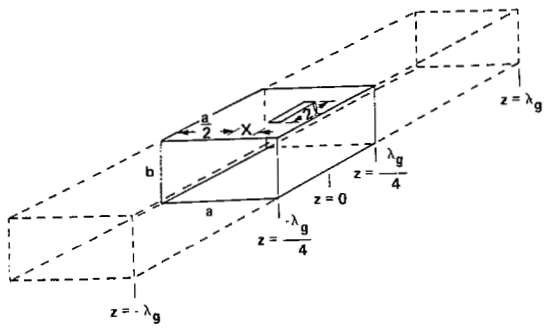

Fig. 1. Waveguide/slot module.

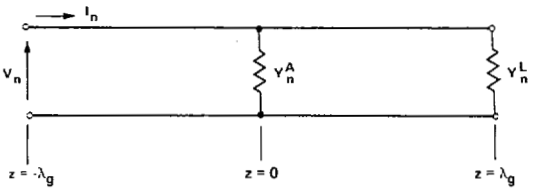

Fig. 2. Equivalent circuit of nth module.

admittance $Y_n{}^L$ is placed at the output port ($z = +\lambda_g$). This admittance (transformed through $3\lambda_g/4$) could represent what the nth module "sees" looking down its branch line at all the modules beyond, or it could be an appropriate termination, such as an open circuit. $Y_n{}^A$ is the active admittance of the nth slot. It is an important parameter in this analysis and its meaning can be appreciated by considering the interrelations among all the modules.

To account for mutual coupling, one can write

$$I_n = \sum_{m=1}^{N} V_m Y_{mn} \tag{1}$$

in which Y_{mn} is the mutual admittance between the input ports m and n. Y_{nn} is the self-admittance of port n; that is,

$$Y_{nn} = Y_n + Y_n{}^L \tag{2}$$

in which Y_n is the value that $Y_n{}^A$ would assume if all other input ports were short-circuited. Y_n is commonly called the self-admittance of the nth slot.

Generally, the input admittance at the nth port is

$$Y_n{}^{in} = \frac{I_n}{V_n} = Y_n{}^A + Y_n{}^L = \sum_{m=1}^{N} \frac{V_m}{V_n} Y_{mn}$$

$$= Y_{nn} + \sum_{m=1}^{N}{}' \frac{V_m}{V_n} Y_{mn} = Y_n + Y_n{}^L + \sum_{m=1}^{N}{}' \frac{V_m}{V_n} Y_{mn} \tag{3}$$

in which the prime on the summation sign means that the term $m = n$ has been excluded. It follows that

$$Y_n{}^A = Y_n + \sum_{m=1}^{N}{}' \frac{V_m}{V_n} Y_{mn}. \tag{4}$$

In words, (4) states that the active admittance at the terminals of the nth module equals the self-admittance of the nth slot plus a term which accounts for mutual coupling. This latter term is a summation which involves not only the mutual admittances between ports, but also the relative voltages at the different ports. As the analysis develops further, it will be seen that $Y_n{}^A$ is decisive in determining the amplitude and phase of the electric field in the nth slot. Since the latter is dictated by the desired radiation pattern, $Y_n{}^A$ becomes the focal point of array design.

It is well known that the scattering off a shunt element is symmetrical and given by

$$B = C = -\frac{1}{2} \frac{Y_n{}^A}{G_0} V_n \tag{5}$$

in which B and C are the amplitudes of the back and forward TE_{10} scattered modes. In the manner of Stevenson [1], one can show that B is related to the slot voltage $V_n{}^S$ by the equation

$$B = -j \left[\frac{2}{\pi^2 \eta G_0} \cdot \frac{(a/b)}{(\beta/k)} \right]^{1/2} \sin \frac{\pi x_n}{a} (\cos \beta l_n - \cos k l_n) V_n{}^S \tag{6}$$

wherein $k = 2\pi/\lambda_0$, and η is the impedance of free space; a and b are the interior dimensions of the rectangular waveguide.

When (5) and (6) are combined, one obtains

$$V_n = \frac{1}{Y_n{}^A/G_0} \left\{ j \left[\frac{8}{\pi^2 \eta G_0} \cdot \frac{(a/b)}{(\beta/k)} \right]^{1/2} \cdot \sin \frac{\pi x_n}{a} (\cos \beta l_n - \cos k l_n) \right\} V_n{}^S. \tag{7}$$

It will be seen shortly that (7) is one of the two principal design equations which emerge from the analysis. A study of (7) reveals that the mode voltage and slot voltage are in phase quadrature if $Y_n{}^A/G_0$ is pure real. In most slot array design problems, $V_n{}^S$ is governed by the pattern requirements and V_n is a common voltage in any given branch line. Thus if all the $V_n{}^S$ slot voltages are to be in phase with each other, and all the mode voltages V_n are to be in phase with each other, it follows that all the active admittances $Y_n{}^A$ should have a common phase. A simple choice is to require that all $Y_n{}^A$ be pure real. But a study of (4) indicates that, if $Y_n{}^A$ is to be pure real, in general Y_n, the self-admittance of the nth slot, will *not* be pure real. In other words, when mutual coupling is taken into account, one cannot expect the resonant self-conductance data will be pertinent in the design. Indeed, in many practical applications, the requisite value of Y_n can be quite far off resonance.

The other principal design equation arises from linking the performance of the slot array to that of an equivalent dipole array via Babinet's principle. Clearly, if the usual assumption of an infinite perfectly conducting ground plane is made, and if the feeding currents of the center-fed strip dipoles match the slot voltages of the slots, the patterns will be essentially the same. To get the impedance characteristics to match also, one needs to place a load impedance $Z_n{}^L$ in series with the nth

equivalent dipole to account for the fact that the resonant length of the slot is affected by its offset, whereas no corresponding effect exists for the dipole. When this is done and complex powers are equated for corresponding elements in the two arrays, it can be shown [2] that

$$\frac{Y_n{}^A}{G_0} = \frac{1}{Z_n{}^A/73}\left\{\frac{4(a/b)}{0.61\pi(\beta/k)}(\cos\beta l_n - \cos kl_n)^2 \sin^2\frac{\pi x_n}{a}\right\}. \tag{8}$$

In (8), $Z_n{}^A$ is the active impedance of the nth strip dipole, defined by

$$Z_n{}^A = Z_n + Z_n{}^L + \sum_{m=1}^{N}{}' \frac{I_m}{I_n} Z_{mn}, \tag{9}$$

wherein Z_n is the self-impedance of the dipole, $Z_n{}^L$ is the load impedance placed in series with it, Z_{mn} is the conventional mutual impedance between dipoles calculable from formulas such as those of Baker and LaGrone [3], and I_m/I_n is the aperture distribution. Thus if the pattern requirement is known (so that I_m/I_n is known), and if $(Z_n + Z_n{}^L)$ is known as a function of x_n and l_n (this relation will be deduced shortly), then $Z_n{}^A$ can be calculated, placed in (8), and $Y_n{}^A/G_0$ can be determined.

Equation (8) permits the interesting interpretation that the normalized active admittance of a longitudinal shunt slot is equal to Stevenson's expression for the resonant normalized conductance (the factor in curly brackets) divided by the active impedance of the corresponding loaded dipole normalized to 73 Ω.

Equation (8) also applies for the case of an isolated slot, in which case $Z_n{}^A$ reduces to $Z_D + Z_L$, with Z_D the self-impedance of the isolated strip dipole and Z_L the load impedance in series with it whose presence models the reactive effects of internal higher order mode scattering off the slot due to its offset. This serves to point up some of the limitations of Stevenson's original expression. Not only does it apply only for resonant length slots, but strictly it becomes a less accurate approximation as the slot width and/or its offset is increased. This is because Z_D is affected by the width of the strip dipole, and Z_L is affected by the offset of the slot.

Equation (8) can be partitioned [2] to yield the first-order results

$$\frac{Y_n}{G_0} = \frac{\left\{\frac{4(a/b)}{0.61\pi(\beta/k)}(\cos\beta l_n - \cos kl_n)^2 \sin^2\frac{\pi x_n}{a}\right\}}{(Z_{nn}/73) - \sum_{m=1}^{N}{}' (Z_{mn}/73)^2/(Z_{mm}/73)} \tag{10}$$

$$\frac{Y_{mn}}{Y_n} = -\frac{Z_{mn}}{Z_{mm}} \cdot \frac{(\cos\beta l_m - \cos kl_m)\sin\frac{\pi x_m}{a}}{(\cos\beta l_n - \cos kl_n)\sin\frac{\pi x_n}{a}}. \tag{11}$$

Equation (11) leads to the interesting conclusion that

$$\frac{Y_{mn}{}^2}{Y_m Y_n} = \frac{Z_{mn}{}^2}{Z_{mm}Z_{nn}}. \tag{12}$$

When use is made of (10)–(12), it is important to remember that Y_n, Y_{mn} are admittances associated with the *mode* voltages in the slot array, and that, whereas Z_{mn} is the conventional mutual impedance between dipoles, Z_{nn} is the *loaded* self-impedance of the nth dipole since it contains $Z_n{}^L$.

EXPERIMENT

If the foregoing theory is valid, the proper design of a one- or two-dimensional longitudinal shunt slot array involves the choice of offsets and lengths for the various slots such that (7) and (8) are simultaneously satisfied for all values of n. One begins by knowing the desired aperture distribution ($V_m{}^S/V_n{}^S$ for the slots, or I_m/I_n for the equivalent dipoles) and the relative mode voltages V_m/V_n (these would all be the same in a standing wave linear array, but would depend on the selection of main-line/branch-line coupling coefficients in a planar array). Then knowledge of the function $Z_n{}^A(x_1, \cdots, x_N, l_1, \cdots, l_N)$ permits determination of all the lengths and offsets such that the desired aperture distribution is achieved, and such that the individual values of $Y_n{}^A/G_0$ cause the branch line admittances and main line admittances to add up to give the desired match.

A key ingredient in this process is to find the function $Z_n{}^A(x_1, \cdots, x_N, l_1, \cdots, l_N)$. As mentioned earlier, the mutual part of $Z_n{}^A$ can be calculated from conventional formulas if the aperture distribution is specified. Now we turn our attention to the determination of the self-part of $Z_n{}^A$, namely $(Z_n + Z_n{}^L)$. If we assume that $(Z_n + Z_n{}^L)$ is essentially the same whether the other dipoles are present and open circuited, or absent, then $(Z_n + Z_n{}^L) = (Z_{\mathrm{SELF}} + Z_{\mathrm{LOAD}})$; that is, it equals the loaded self-impedance of an isolated dipole (corresponding to an isolated slot). But for this case (8) becomes

$$Z_{\mathrm{SELF}} + Z_{\mathrm{LOAD}} = \frac{73}{Y_{\mathrm{SELF}}/G_0}\left\{\frac{4(a/b)}{0.61\pi(\beta/k)}(\cos\beta l_n - \cos kl_n)^2 \sin^2\frac{\pi x_n}{a}\right\}. \tag{13}$$

Regardless of the shape of the slot (rectangular, rounded ends, dumbbell, etc.), if one *measures* Y_{SELF}/G_0 as a function of offset x and length l, (13) can be used to express $(Z_n + Z_n{}^L)$ as a function of x_n and l_n. This can then be used in (8) for *all* aperture distributions and feeding arrangements. For rectangular slots, the *theoretical* values of Y_{SELF}/G_0 obtained by the method of Khac [4] can be used in lieu of experimentally obtained information.

It is desirable to accumulate the data on Y_{SELF}/G_0 in the universal form discovered by Stegen [5] and illustrated in Fig. 9-5 of Jasik [6]. This figure shows plots of the real and imaginary parts of $Y_{\mathrm{SELF}}/G_0 \div G_{\mathrm{RES}}/G_0$ versus l/l_{RES}. The range of greatest use in the design of slot arrays is $0.95 < l/l_{\mathrm{RES}} < 1.05$ and the theoretical work of Khac [4] supports the assumption of universality in this range. Fig. 9-5 of Jasik requires his companion Figs. 9-6 and 9-7, in which G_{RES}/G_0 and $2l_{\mathrm{RES}}/\lambda_0$ are plotted as functions of slot offset. When polyfits are made

to the four curves in Fig. 9-5, 6, and 7 of Jasik, $(Z_n + Z_n^L)$ can be expressed in a form easily handled by a computer.

Fig. 9-7 of Jasik leads to a first test of the theory. Stegen dealt with round ended slots in a wall 0.050 in thick. The question arises as to the length of the equivalent strip dipole of rectangular contour in a wall of "zero" thickness. This can be determined by the following argument. As the offset $x \to 0$, the amplitudes of all the modes scattered off the slot tend to zero. With respect to higher order mode scattering, this has the implication for the complementary dipole that its loading impedance tends to zero also. But in this circumstance, (13) indicates that Z_{SELF} should be pure real for the dipole when Y_{SELF} is pure real for the slot. Tai has shown [7] that a strip dipole of width w and negligible thickness is equivalent to a cylindrical dipole of diameter $d = w/2$. Tai also provides a convenient formula [7] for the impedance of a cylindrical dipole as a function of its length $2l$ and its radius $a = d/2$. Since Stegen used slots 0.0625 in wide, if one places $a = 0.0156$ in in Tai's formula, one can deduce that $2l_r/\lambda_0 = 0.464$, wherein $2l_r$ is the resonant length of the unloaded strip dipole. On the other hand, a study of Fig. 9-7 of Jasik reveals that Stegen's asymptotic value is $2l_r^\circ/\lambda_0 = 0.483$, in which $2l_r^\circ$ is the resonant length of his round ended slot at zero offset. From this it follows that $f = 2l_r^\circ/2l_r = 1.04$. This length adjustment factor is in agreement with the findings of Oliner [8], who attributes a 2 percent correction for round ends and a 2 percent correction for wall thickness in this situation.

When the foregoing theory is used to design slot arrays, the procedure just described can be utilized to determine the length adjustment factor f. Experience shows that f is quite sensitive to the b dimension of the waveguide, as well as to wall thickness.

A second test involves a prediction of resonant conductance versus offset for an isolated slot. Since the higher order mode scattering off this slot is nonpropagating and thus contributes primarily to the storage of reactive energy, it seems reasonable to assume that the load impedance Z_L possesses a small resistive component R_L. In practical circumstances, the dipole self-impedance Z_D has a resistive component in the neighborhood of 73 Ω, and thus one should expect that $R_L \ll R_D$. For a resonant slot $X_L = -X_D$, and in this case (8) can be approximated by

$$\frac{G_r}{G_0} = \frac{73}{R_D}\left\{\frac{4(a/b)}{0.61\pi(\beta/k)}(\cos \beta l_r - \cos kl_r)^2 \sin^2 \frac{\pi x}{a}\right\}. \quad (14)$$

For standard X-band guide, a frequency of 9.375 GHz, and a length adjustment factor $f = 1.04$, (14) yields the solid curve found in Fig. 3. Stegen's experimental points are shown for comparison.

It should be recognized that the agreement seen between theory and experiment in Fig. 3 is not a case of adjusting a parameter in the theoretical formula to get curve fitting. All that has been done in (14) is to ignore R_L and assume that the equivalent dipole is resonant. A plot of the original Stevenson formula would lie 20 percent below the solid curve of Fig. 3 at the low end, and 10 percent below it at the high end.

A third test involving an isolated slot concerns the frequency dependence of resonant conductance. Stegen [5] found experimentally that his curve of resonant length versus offset for a longitudinal shunt slot (Fig. 9-7 of Jasik) is universal in the sense that if the offset remains constant, $2l_r^\circ/\lambda_0$ also remains essentially constant even though the frequency varies. This has

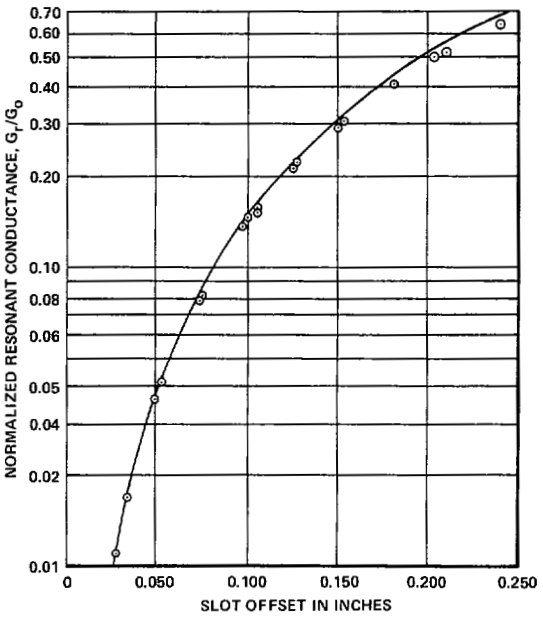

Fig. 3. G_r/G_0 for resonant longitudinal slot versus offset 9.375 GHz, $a = 0.900$ in, $b = 0.400$ in, slot width = 0.0625 in, wall thickness = 0.050 in. Points are Stegen's measured values; curve is theoretical.

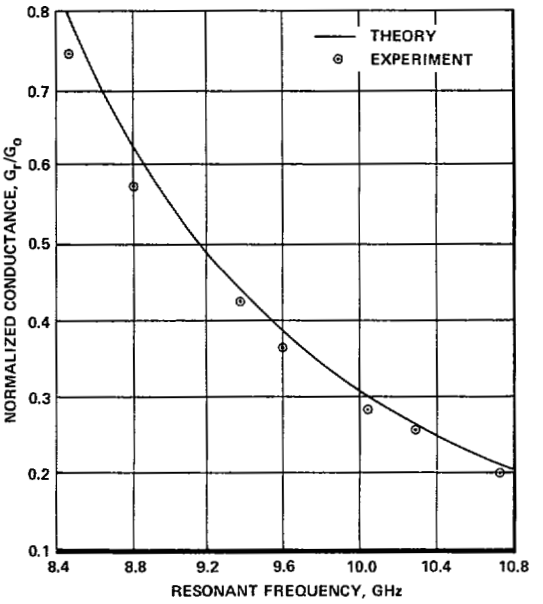

Fig. 4. Resonant conductance versus frequency.

the implication that if kl_r remains constant in (14), that is, the slot length is continually adjusted as the frequency is changed so as to maintain resonance, then for a slot of a given offset, G_r/G_0 is a function of frequency only because β/k varies with frequency. For a slot of offset 0.183 in, (14) yields the solid curve shown in Fig. 4. Stegen's experimental data points are shown for comparison.

Now let us consider situations involving more than just one isolated slot. As a first step, an array of two slots, one each in two parallel waveguides, with the slots staggered longitudinally a quarter of a guide wave-length, was constructed with the dimensions shown in Fig. 5 and imbedded in an 8-in by 10-in ground plane. This array was used to test the validity of (10)–(12) in the following way. With one slot covered over

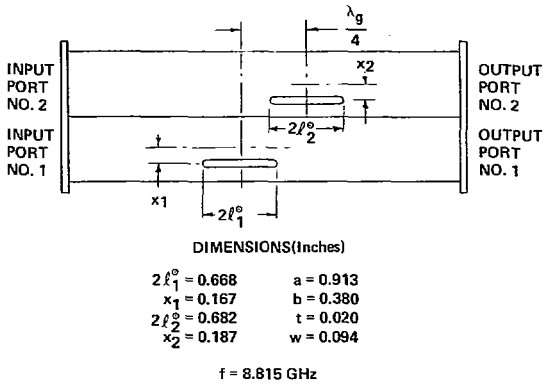

Fig. 5. Two-slot array.

TABLE I
MEASURED AND COMPUTED DATA FOR TWO-SLOT ARRAY

Quantity	Measured Value	Computed Value
Y_1/G_o (Isolated)	0.52 + j 0.065	
Y_2/Go (Isolated)	0.62 + j 0.065	
Z_{11}		63.93 - j 7.99
Z_{22}		69.79 - j 7.32
Z_{12}		-16.32 + j 4.40
Y_1/G_o	0.58 + j 0.05	0.56 + j 0.06
Y_2/G_o	0.64 + j 0.05	0.66 + j 0.06
Y_{12}/G_o	$0.146 \angle -4.2^\circ$	$0.153 \angle -3.1^\circ$

with conducting tape, a short circuit was placed $3\lambda_g/4$ beyond the other slot, and a measurement was taken of its input admittance. This resulted in the data shown in the first two rows of Table I. A length contraction factor $f = 1.03$ was found to apply for this configuration and used to determine l_1 and l_2. Equation (8) then gave

$$Z_{11} = \frac{33.76}{Y_1/G_0 \text{ (isolated)}} \qquad Z_{22} = \frac{43.72}{Y_2/G_0 \text{ (isolated)}} \tag{15}$$

from which the entries in the third and fourth rows of Table I were obtained.

Z_{11} and Z_{22} as they appear in (15) are the loaded self-impedances of the strip dipoles equivalent to each isolated slot. Strictly speaking, they are not the same as the quantities one should use when other dipoles are present but open-circuited; however, at this slot spacing the approximation is a good one, and therefore the entries for Z_{11} and Z_{22} in Table I will be used in (10)–(12).

The calculation of mutual dipole impedance was made using the formulas of Baker and LaGrone [3], and provides the fifth row entry in Table I.

Equation (10) predicts that if the conducting tape covering the second slot is removed and replaced by a short circuit λ_g from the center of the second slot, and then the input admittance of the first slot is measured, the result should satisfy

$$\frac{Y_1}{G_0} = \frac{33.76}{Z_{11} - (Z_{12}^2/Z_{22})} \qquad \frac{Y_2}{G_0} = \frac{43.72}{Z_{22} - (Z_{12}^2/Z_{11})}. \tag{16}$$

When the values listed in Table I for Z_{11}, Z_{22}, and Z_{12} are used in (16), computed values of Y_1/G_0 and Y2/G0 can be ascertained. These values have been entered in the sixth and seventh rows of Table I. The measured values are listed alongside for comparison.

Finally, (12) of the theory can be put in the form

$$\frac{Y_{12}}{G_0} = \left[\frac{Y_1}{G_0} \cdot \frac{Y_2}{G_0} \cdot \frac{Z_{12}^2}{Z_{11}Z_{22}}\right]^{1/2}. \tag{17}$$

When the various computed values found in Table I are inserted in (17), the prediction is that $Y_{12}/G_0 = 0.153 \angle -3.1^\circ$.

The accurate measurement of Y_{12}/G_0 is difficult. After some experimentation, the following procedure was adopted. Short circuits were placed $3\lambda_g/4$ beyond each slot. Slotted lines were put in tandem with both input ports. A variable attenuator was placed before one slotted line, and a variable phase shifter before the other. The two branches were fed through a conventional T junction. But from (4),

$$\frac{Y_1^A}{G_0} = \frac{Y_1}{G_0} + \frac{V_2}{V_1}\frac{Y_{12}}{G_0} \qquad \frac{Y_2^A}{G_0} = \frac{Y_2}{G_0} + \frac{V_1}{V_2}\frac{Y_{12}}{G_0}. \tag{18}$$

It follows that one can select the attenuator setting such that $|V_1/V_2| = 1$. If then the phase of V_1/V_2 is varied, Y_1^A/G_0 and Y_2^A/G_0 will have loci which are circles of the same size, centered around Y_1/G_0 and Y_2/G_0, respectively. The radius of these two equal circles is $|Y_{12}/G_0|$. The phase of the mutual admittance can be determined from corresponding points on the two loci.

This experimental procedure resulted in the Smith chart shown in Fig. 6. From this data, the average measured value of mutual admittance was deduced to be $Y_{12}/G_0 = 0.146 \angle -4.2^\circ$.

Lastly, let us consider the application of (7) and (8) to the design of a two-dimensional array. The procedure can be outlined as follows.

a) Select the frequency of operation and the waveguide dimensions.
b) Deduce the length contraction factor f. This can be done as in the earlier discussion of resonant length for zero offset.
c) Specify the slot voltage distribution needed to get the desired pattern and the sum of the active admittances desired in each branch line waveguide.
d) Solve (7) and (8) simultaneously to give those values of x_n and l_n which satisfy the required aperture distribution and admittance level.

When the above procedure was applied to the design of a two-by-four array, the results were as shown in Fig. 7. The specified admittance level was

$$\sum_{n=1}^{4} Y_n^A/G_0 = \sum_{n=5}^{8} Y_n^A/G_0 = 2 + j0. \tag{19}$$

The measured values were

$$\sum_{n=1}^{4} Y_n^A/G_0 = 1.90 + j0 \qquad \sum_{n=5}^{8} Y_n^A/G_0 = 1.94 + j0. \tag{20}$$

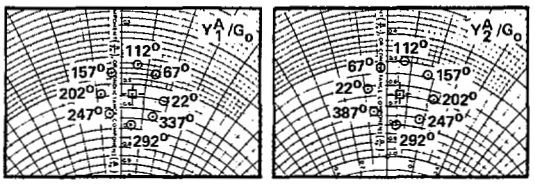

Fig. 6. Active admittance loci for two-slot array.

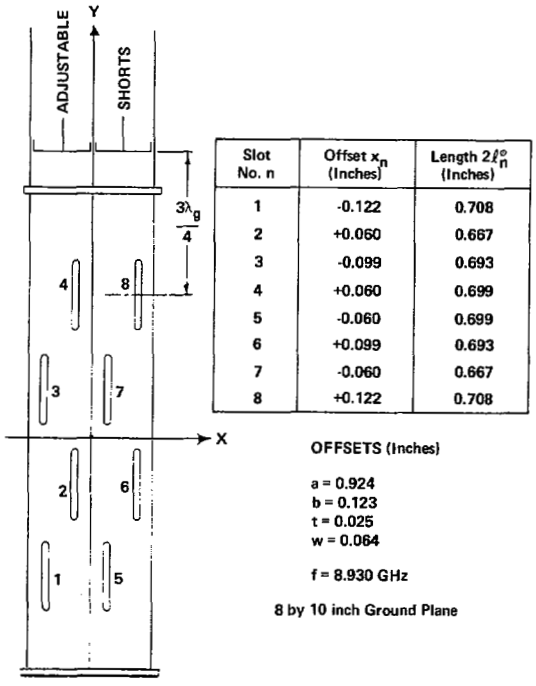

Slot No. n	Offset x_n (Inches)	Length $2\ell_n^\circ$ (Inches)
1	-0.122	0.708
2	+0.060	0.667
3	-0.099	0.693
4	+0.060	0.699
5	-0.060	0.699
6	+0.099	0.693
7	-0.060	0.667
8	+0.122	0.708

OFFSETS (Inches)

a = 0.924
b = 0.123
t = 0.025
w = 0.064

f = 8.930 GHz

8 by 10 inch Ground Plane

Fig. 7. Two-by-four slot array.

The specified aperture distribution was uniform amplitude/uniform phase, so the predicted pattern has a broadside beam, symmetrical sidelobes, and a 13.5-dB sidelobe level. The experimental *H*-plane pattern is shown in Fig. 8.

A study of the table of slot lengths and offsets (Fig. 7) reveals several interesting and surprising things. First, there is a 2:1 range in slot offsets. (Were one to ignore mutual coupling, or include it but ignore its variability from slot to slot, all offsets would be the same.) Second, no slot in this array is self-resonant; each slot is detuned appropriately to make the individual *active* admittance resonant. Third, there is a quadrant I/quadrant III and quadrant II/quadrant IV symmetry to the lengths and offsets, but no symmetry around the X axis nor around the Y axis. This can be traced to nonsymmetrical effects caused by staggering the offsets.

The range of lengths and offsets found for this two-by-four array illustrates the general observation that small arrays present a more difficult design problem than do large arrays. In the latter, only elements near an edge "see" a different mutual coupling environment, so achieving the proper active admittance becomes simpler. Further, mechanical and electrical tolerances ease off as the array gets larger [9].

Though the details are not being reported here, the above procedure has been used successfully to design a 12-slot linear array for a 30 dB side lobe level, a 19-slot linear array for asymmetric side lobes (all at 20 dB except the inner three on one side of the main beam at 30 dB) and a 52-element two-dimensional slot array with a uniform aperture distribution.

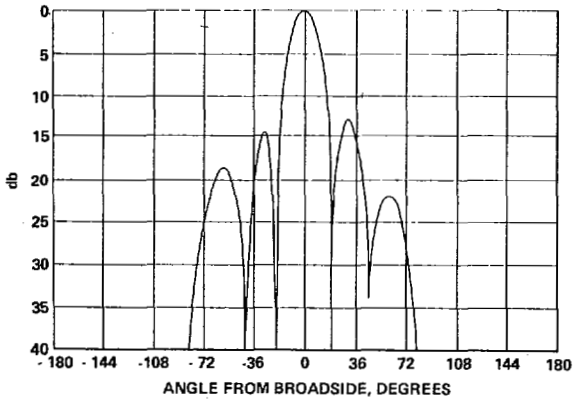

Fig. 8. *H*-plane pattern of two-by-four array described in Fig. 7, $f = 8.933$ GHz.

CONCLUSIONS

A theory has been presented which can account for the array behavior of longitudinal shunt slots in terms of the characteristics of complementary dipoles. Formulas for active, self-, and mutual admittances of longitudinal slots have been derived. Slot arrays can be designed by choosing the lengths and offsets of individual slots such that (7) yields a slot voltage distribution consistent with the desired pattern, and such that (8) yields an active admittance distribution consistent with the feed and match requirements of the array.

The analysis can be repeated, in a step-by-step analog, for the case of inclined series slots in the broad wall of rectangular waveguides. It can also be extended to arrays of strip-line-fed slots.

The theory has been tested experimentally in a variety of situations involving a single slot, a pair of slots, and a small two-dimensional array. In general, the agreement has been found to be quite satisfactory.

REFERENCES

[1] A. F. Stevenson, "Theory of slots in rectangular waveguides," *J. Appl. Phys.*, vol. 19, pp. 24–38; Jan. 1948.

[2] R. S. Elliott, "Longitudinal shunt slots in rectangular waveguide: Part I, theory," Rantec, Calabasas, CA, Rantec Report No. 72022-TN-1.

[3] H. C. Baker and A. H. LaGrone, "Digital computation of the mutual impedance between thin dipoles," *IEEE Trans. Antennas Propagat.*, vol. AP-10, pp. 172–178, Mar. 1962.

[4] T. Vu Khac, "A study of some slot discontinuities in rectangular waveguides," Ph.D. dissertation, Monash University, Australia, Nov. 1974.

[5] R. J. Stegen, "Longitudinal Shunt Slot Characteristics," Hughes Technical Memorandum No. 261, Culver City, CA. Nov., 1951.

[6] H. Jasik, *Antenna Engineering Handbook.* New York: McGraw-Hill, 1961, Chapter 9.

[7] C. T. Tai, "Characteristics of linear antenna elements," in *Antenna Engineering Handbook*, H. Jasik, Ed. New York: McGraw-Hill, 1961, Chapter 3.

[8] A. A. Oliner, "The impedance properties of narrow radiating slots in the broad face of rectangular waveguide," *IEEE Trans. Antennas Propagat.*, vol. AP-5, pp. 4–20, Jan., 1957.

[9] R. S. Elliott, "Mechanical and electrical tolerances for two-dimensional scanning antenna arrays," *IRE Trans. Antennas Propagat.*, vol. AP-6, pp. 114–120; 1958.

如 何 学 习 天 线 设 计

天线设计理论晦涩高深，让许多工程师望而却步，然而实际工程或实际工作中在设计天线时却很少用到这些高深晦涩的理论。实际上，我们只需要懂得最基本的天线和射频基础知识，借助于 HFSS、CST 软件或者测试仪器就可以设计出工作性能良好的各类天线。

易迪拓培训(www.edatop.com)专注于微波射频和天线设计人才的培养，推出了一系列天线设计培训视频课程。我们的视频培训课程，化繁为简，直观易学，可以帮助您快速学习掌握天线设计的真谛，让天线设计不再难…

HFSS 天线设计培训课程套装

套装包含 6 门视频课程和 1 本图书，课程从基础讲起，内容由浅入深，理论介绍和实际操作讲解相结合，全面系统的讲解了 HFSS 天线设计的全过程。是国内最全面、最专业的 HFSS 天线设计课程，可以帮助你快速学习掌握如何使用 HFSS 软件进行天线设计，让天线设计不再难…

课程网址：http://www.edatop.com/peixun/hfss/122.html

CST 天线设计视频培训课程套装

套装包含 5 门视频培训课程，由经验丰富的专家授课，旨在帮助您从零开始，全面系统地学习掌握 CST 微波工作室的功能应用和使用 CST 微波工作室进行天线设计实际过程和具体操作。视频课程，边操作边讲解，直观易学；购买套装同时赠送 3 个月在线答疑，帮您解答学习中遇到的问题，让您学习无忧。

详情浏览：http://www.edatop.com/peixun/cst/127.html

13.56MHz NFC/RFID 线圈天线设计培训课程套装

套装包含 4 门视频培训课程，培训将 13.56MHz 线圈天线设计原理和仿真设计实践相结合，全面系统地讲解了 13.56MHz 线圈天线的工作原理、设计方法、设计考量以及使用 HFSS 和 CST 仿真分析线圈天线的具体操作，同时还介绍了 13.56MHz 线圈天线匹配电路的设计和调试。通过该套课程的学习，可以帮助您快速学习掌握 13.56MHz 线圈天线及其匹配电路的原理、设计和调试…

详情浏览：http://www.edatop.com/peixun/antenna/116.html

关于易迪拓培训：

易迪拓培训(www.edatop.com)由数名来自于研发第一线的资深工程师发起成立，一直致力和专注于微波、射频、天线设计研发人才的培养；后于 2006 年整合合并微波 EDA 网(www.mweda.com)，现已发展成为国内最大的微波射频和天线设计人才培养基地，成功推出多套微波射频以及天线设计经典培训课程和 ADS、HFSS 等专业软件使用培训课程，广受客户好评；并先后与人民邮电出版社、电子工业出版社合作出版了多本专业图书，帮助数万名工程师提升了专业技术能力。客户遍布中兴通讯、研通高频、埃威航电、国人通信等多家国内知名公司，以及台湾工业技术研究院、永业科技、全一电子等多家台湾地区企业。

我们的课程优势：

※ 成立于 2004 年，10 多年丰富的行业经验

※ 一直专注于微波射频和天线设计工程师的培养，更了解该行业对人才的要求

※ 视频课程、既能达到了现场培训的效果，又能免除您舟车劳顿的辛苦，学习工作两不误

※ 经验丰富的一线资深工程师主讲，结合实际工程案例，直观、实用、易学

联系我们：

※ 易迪拓培训官网：http://www.edatop.com

※ 微波 EDA 网：http://www.mweda.com

※ 官方淘宝店：http://shop36920890.taobao.com